*International Journal of Fracture* **100**: 121–131, 1999.


# Modeling of development of localized plastic deformation and prefracture stage in mesovolumes of heterogeneous media

P.V. MAKAROV, I.Y. SMOLIN, I.P. PROKOPINSKY and YU.P. STEFANOV
*Institute of Strength Physics and Materials Science of Siberian Branch of Russian Academy of Sciences, Tomsk 634021, Russia; e-mail: pvm@ispms.tsc.ru*

Received 9 February 1999; accepted in revised form 23 March 1999

**Abstract.** Mesovolumes of materials are the objects of investigation in this paper. These volumes containing significant elements of internal structure of material are investigated by numerical methods of continuous media mechanics. The purpose of the research is numerical modeling of localized deformation at the mesoscale. Results of the calculations show that joint influence of heterogeneities of internal structure of material and action of maximum shear stresses results in localized development of plastic deformation as a system of shear bands. They are accompanied by formation of bulk structural elements, which move as units relatively to each other. It is shown that rotations in the regions of strain localization are higher than those in the other parts of the specimen.

**Key words:** Plastic deformation localization, numerical modeling, mesoscale, shear bands.

## 1. Introduction

The traditional approaches of fracture mechanics based on the averaged description at macroscopic scale consider problems of development and propagation of individual cracks. The prefracture stage precedes such processes. It is characterized by formation and accumulation of damages and microcracks at lower scale levels – micro- and mesoscale. Development of deformation and fracture at the macroscale is determined directly by processes at the meso-level. Experiments show that localization of plastic deformation takes place at the mesoscale at the prefracture stage.

The adequate description and numerical simulation of features of deformation and fracture of materials under various kind of loading are of great importance to the problem of design of advanced materials. It is well known from experiments (Nadai, 1950; Panin, 1990) that plastic deformation is generated irregularly and its development is accompanied with formation of various regions of localized strain of different scales at prefracture stage. At meso and macro levels there are shear bands, thinning regions, Lüders bands, neck formation, etc. The subject of this paper is the problem of computer simulation of the phenomena of a similar nature.

The approach of mesomechanics of solids, the conception of scale and structural levels of deformation and fracture are used here (Panin, 1990; 1998). Just at the mesoscale there are basic features of plastic deformation not investigated yet. By mesovolume we mean a volume of a material in which we explicitly deal with heterogeneities of internal structure having various physical-mechanical properties. In such mesovolumes of material a medium is nonhomogeneous. It has a structure which evolve in course of loading. Some heterogeneities of the structure can be taken into account explicitly whereas other ones can be included non explicitly by using various complexifications of the continuous medium model. Heterogeneity of internal structure of a material causes heterogeneity of the stressed-strained state in the

material under loading. The main features of stressed-strained state observed in experiments should be received in simulations.

Some problems of finite element analysis of mesovolumes of polycrystalline Ag and also fiber and particle reinforced composites under deformation are presented in papers of S. Schmauder with co-workers (Soppa et al., 1998; Dong, 1996). Numerical aspects of shear band formation in single crystals and polycrystals with respect to crystallographic orientation are investigated partially in (Dène et al., 1988; Harren et al., 1988). Unlike mentioned papers, here finite difference analysis of model mesovolumes of different materials is carried out. We use simple isotropic elastic perfectly plastic model and pay especial attention on inhomogeneity of materials at the mesolevel. Though quasi-static loading is considered, dynamic numerical method is applied.

## 2. Model and method of simulation

The Lagrange approach is adopted. Two-dimensional problems under plane strain and plane stress conditions are considered. The set of equations for the case of two dimensional plane elastic-plastic flow with the von Mises yield criterion will be used (Wilkins, 1964; Wilkins and Guinan, 1976).

With reference to the space coordinates $(x, y)$, relations for the strain rates are given by

$$\dot{\varepsilon}_{xx} = \frac{\partial v_x}{\partial x}, \qquad \dot{\varepsilon}_{yy} = \frac{\partial v_y}{\partial y}, \qquad \dot{\varepsilon}_{xy} = \frac{1}{2}\left(\frac{\partial v_y}{\partial x} + \frac{\partial v_x}{\partial y}\right), \tag{1}$$

where $v_x$ and $v_y$ are the velocities in $x$- and $y$-direction, respectively, the dot over a parameter means a time derivative. Note that $\dot{\varepsilon}_{zz} = \dot{h}/h$ for plane stress and $\varepsilon_{zz} = 0$ for plane strain, where $h$ denotes the plate thickness and $z$ is coordinate along the thickness direction. The rotation rate is given by

$$\dot{\omega}_z = -\dot{\omega}_{xy} = \frac{1}{2}\left(\frac{\partial v_y}{\partial x} - \frac{\partial v_x}{\partial y}\right). \tag{2}$$

The equations of motion in plane $x$-$y$ coordinates have the form

$$\rho\frac{\partial v_x}{\partial t} = \frac{\partial \sigma_{xx}}{\partial x} + \frac{\partial \sigma_{xy}}{\partial y}, \qquad \rho\frac{\partial v_y}{\partial t} = \frac{\partial \sigma_{xy}}{\partial x} + \frac{\partial \sigma_{yy}}{\partial y}. \tag{3}$$

Here $\rho$ is the actual mass density, $t$ is the time and $\sigma_{xx}, \sigma_{yy}, \sigma_{xy}, \sigma_{zz}$ are the stress tensor components.

The equation of continuity can be written as

$$\frac{\dot{V}}{V} = \dot{\varepsilon}_{xx} + \dot{\varepsilon}_{yy} + \dot{\varepsilon}_{zz}, \tag{4}$$

where $V = \rho_0/\rho$ is the relative volume and $\rho_0$ is the reference density. Using decomposition of the stresses into the hydrostatic component $P$ and the deviator components $s_{ij}$

$$\sigma_{ij} = -P\delta_{ij} + s_{ij} \tag{5}$$

and decomposition of the strain rates into elastic and plastic parts

$$\dot{\varepsilon}_{ij} = \dot{\varepsilon}^e_{ij} + \dot{\varepsilon}^p_{ij}, \tag{6}$$

it can be written according to the associated relation of plastic flow

$$\dot{\varepsilon}^p_{ij} = \dot{\lambda} s_{ij}. \tag{7}$$

Due to the Hooke's law the relations for the stress deviators are the following

$$\frac{Ds_{xx}}{Dt} = 2\mu\left(\dot{\varepsilon}_{xx} - \frac{1}{3}\frac{\dot{V}}{V}\right) - 2\mu\dot{\lambda}s_{xx}, \tag{8}$$

$$\frac{Ds_{yy}}{Dt} = 2\mu\left(\dot{\varepsilon}_{yy} - \frac{1}{3}\frac{\dot{V}}{V}\right) - 2\mu\dot{\lambda}s_{yy}, \tag{9}$$

$$\frac{Ds_{xy}}{Dt} = 2\mu\dot{\varepsilon}_{xy} - 2\mu\dot{\lambda}s_{xy}. \tag{10}$$

Note that

$$\frac{Ds_{ij}}{Dt} = \dot{s}_{ij} - \dot{\omega}_{ik}s_{kj} + s_{ik}\dot{\omega}_{kj} \tag{11}$$

means the Jaumann time derivative, $\mu$ is the shear modulus and $\dot{\lambda}$ is a scalar plastic flow rate parameter defined by the von Mises yield condition $s^2_{xx} + s^2_{yy} + 2s^2_{xy} + s^2_{zz} = \frac{2}{3}Y^2_0$, where $Y_0$ is the yield strength. For plane stress we have

$$\sigma_{zz} = -P + s_{zz} = 0 \tag{12}$$

and for plane strain we have

$$s_{zz} = -(s_{xx} + s_{yy}). \tag{13}$$

For stresses lower than 1 GPa and barotropic model of medium we can take for the hydrostatic pressure the following relation

$$\dot{P} = -K\frac{\dot{V}}{V}, \tag{14}$$

where $K$ is the bulk modulus of elasticity.

Absence of stresses in calculation region is assumed as initial conditions for the calculations. External loading are assigned, as a rule, by the following boundary conditions. At two opposite edges of the rectangular computational zone smooth increasing of velocities are applied for some initial period of time, after that constant velocities (in order of 1 m/s) are applied until the required integral strain is achieved. At two another opposite edges of computational zone the free surface conditions are set.

For numerical solving this set of equations a numerical technique that is an analogue of well-known finite-difference HEMP method (Wilkins, 1964; Wilkins and Guinan, 1976) is

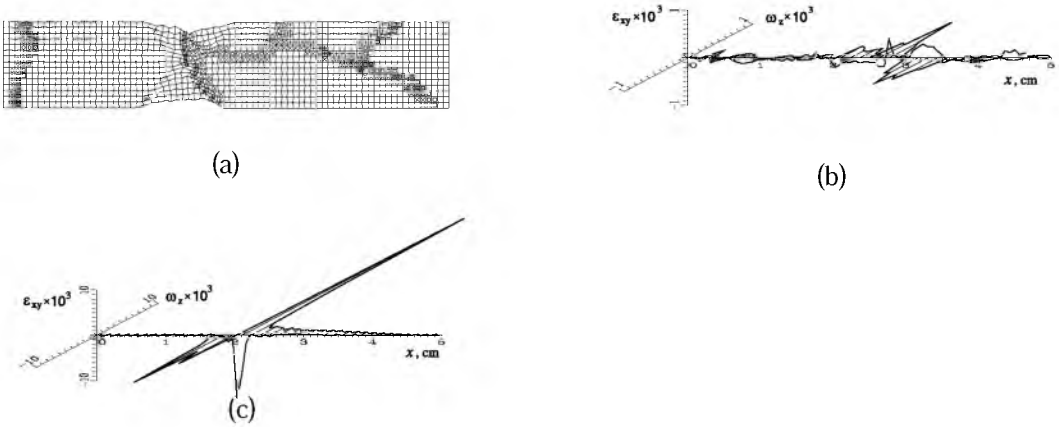


*Figure 1.* Calculation grid for coarse-grained Al sample with 3 percent tensile strain (*a*) and distribution of plastic shear and rotation along the sample axis in different time moments (b)–(c).

used. Uniform square grids are taken. All computations are carried out on personal computer using the computer program based on the method and written by the authors. An algorithm of grid nodes splitting was applied to model fracture (Panin et al., 1995; Gridneva and Nemirovich-Danchenko, 1983).

## 3. Results and discussion

It is interesting to clear up the influence of heterogeneity of a material internal structure at development of localization of plastic deformation in mesovolume. At the beginning let us consider the most simple case when separate fragments of material differ only by strength properties (they have different yield strengths).

Figure 1 shows results of simulation of a coarse-grained aluminum specimen loaded in tension. The problem was solved under plane strain condition. The map of grain structure was taken from one of the coarse-grained specimens prepared for experiments (Panin, 1990). Heterogeneous inner structure was modeled by assuming that yield strengths of different structure fragments: grains and grain boundary regions (the last are indicated by different markers in Figure 1) differ. The yield strengths in the grains themselves $Y_0^*$ were assumed to be larger than those in the boundary regions in this case, and have the following values for the corresponding markers in Figure 1: $\Diamond$ — $Y_0 = 26$ MPa ($Y_0^* = 13$ MPa), $\boxtimes$ — $Y_0 = 30$ MPa ($Y_0^* = 15$ MPa), $\times$ — $Y_0 = 35$ MPa ($Y_0^* = 17$ MPa), $\circ$ — $Y_0 = 15$ MPa ($Y_0^* = 8$ MPa), $+$ — $Y_0 = 20$ MPa ($Y_0^* = 10$ MPa), $\square$ — $Y_0 = 25$ MPa ($Y_0^* = 12$ MPa). The rest material parameters used in the computation are the following: $\mu = 26.2$ GPa, $K = 76.5$ GPa, $\rho = 2.7$ g/cm$^3$. The computation grid contains $76 \times 16$ nodes with initial space step 0.067 cm. It can be seen that two shear bands and neck form. When deforming, two shear bands appear in the regions of fragments of structure with the least strength. In Figure 1(b)–(c) change in shear $\varepsilon_{xy} = 0.5(\partial u_y/\partial x + \partial u_x/\partial y)$ and rotation $\omega_z = 0.5(\partial u_y/\partial x - \partial u_x/\partial y)$ along the axis of the sample is submitted. Here $u_x$ and $u_y$ are the displacements in $x$- and $y$-direction, respectively. Shear and rotation change along the axis periodically and in opposite phases. These results are qualitatively agreed with results of experiments on similar samples (Panin, 1990; 1995). One can see that peak deviations of these values correspond to the zones of strain localization, the change in rotation being larger. It is possible to achieve another location of bands and even one

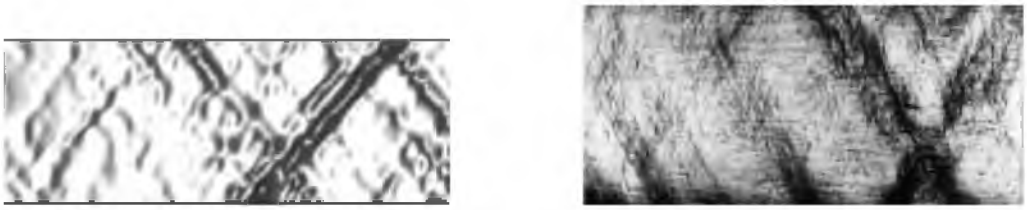

*Figure 2.* Mesobands of localized strain on the surface of thin steel plates. The width of the plates in both figures are equal to 1 cm.

shear band can be formed only for the same sample geometry with other distribution of the characteristics of various elements of internal structure. As subsequent fracture occurs near the bands of localized strain it is very important to reveal them. Rotation seems to be very sensitive to shear band generation. So, surges of rotations allow to reveal regions of strain localization at early stage of localization. Some methods of non-destructive testing are based on this principle (Panin et al., 1993).

A result of other calculation in comparison with experiments of V.E. Panin with co-workers (Panin, et al., 1993) are submitted in Figure 2. There are results of tension test for a plate, high nitrogen steel. So, the calculation for a thin plate where plane stress condition exists were performed. The following material constants were used in the calculation $\mu = 79\,\text{GPa}$, $K = 142.3\,\text{GPa}$, $\rho = 8\,\text{g/cm}^3$. The computation grid contains $60 \times 20$ nodes with initial space step 0.05 cm. The Gaussian distribution of yield strengths was randomly mixed in the calculation grid with disorder of 1 percent ($Y_0 = 300 \pm 3\,\text{MPa}$). The left top figure shows the calculated change in the plate thickness processed specially for comparison with the experimental photo shown in the right picture (Panin, 1995). The dark zones in both pictures correspond to the regions of the sample thinning. Results of calculation show formation of several thinning bands which arrangement coincides with experimental photo. The angles of band inclination to the axis of tension are different in these two cases and also differ from the analytical and calculated values of 55° obtained for homogeneous plate (Nadai, 1950). In this case the alignment and intensity of shear bands are defined by heterogeneity of physical-mechanical properties.

The next example of simulation presents modeling of deformation of representative mesovolume of polycrystalline steel sample. A mesovolume is said to be the representative mesovolume if it has enough amount of structural fragments (grains, in this case) to obtain the properties of material on the macroscale at averaging. So, a representative mesovolume is a point of continuum at the macroscale level. A map of such a representative mesovolume is submitted in Figure 3. It is taken from a real photo for steel. There are more than 120 grains with their average size about 30 $\mu$m in this volume and it can be called representative. In the calculation, material constants were assumed to be the following $\mu = 79\,\text{GPa}$, $K = 142.3\,\text{GPa}$, $\rho = 8\,\text{g/cm}^3$. For fragments of different color (grains) the yield strengths were varied up to 20 percent ($Y_0 = 250 \pm 50\,\text{MPa}$). The computational grid contains $300 \times 298$ nodes with initial space step 1 $\mu$m. In the mesovolume under uniaxial tension along the vertical axis the system of localized strain bands appears with inclination of them about 45° to the axis of tension. In Figure 4 the greater values of effective plastic deformation

$$\varepsilon_v^{pl} = \sqrt{\frac{2}{3}\left(\varepsilon_{xx}^{pl\,2} + \varepsilon_{yy}^{pl\,2} + 2\varepsilon_{xy}^{pl\,2} + \varepsilon_{zz}^{pl\,2}\right)}$$

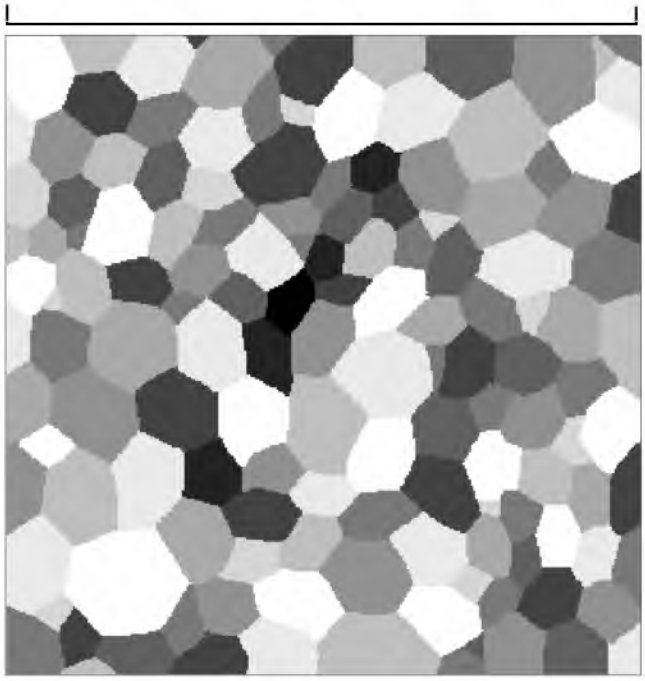

*Figure 3.* Map of representative mesovolume.

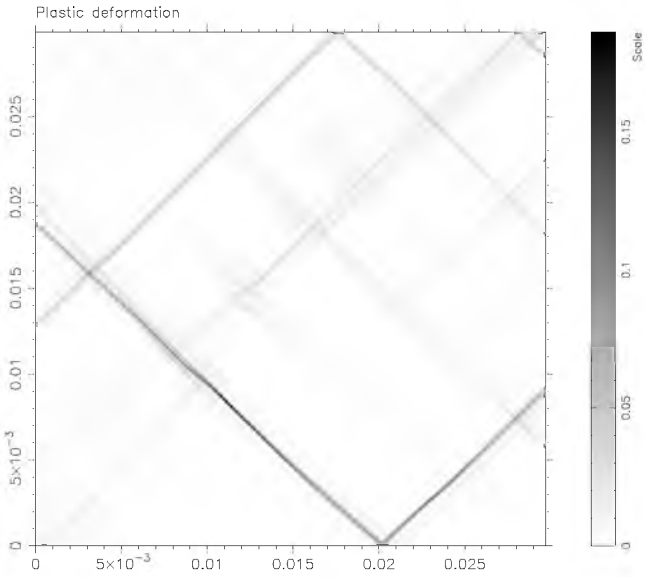


*Figure 4.* Localized strain bands in representative mesovolume.

correspond to the greater intensity of coloring. Deformation in bands, covering on width about 5–8 $\mu$m, ranges up to 30 percent when the integral deformation of the sample is equal to 0.7 percent. The system of bands of localized deformation breaks the sample into separate blocks (bulk structural elements) which move as a whole. This effect of material fragmentation during loading is distinctly seen in the velocity field shown in Figure 5.

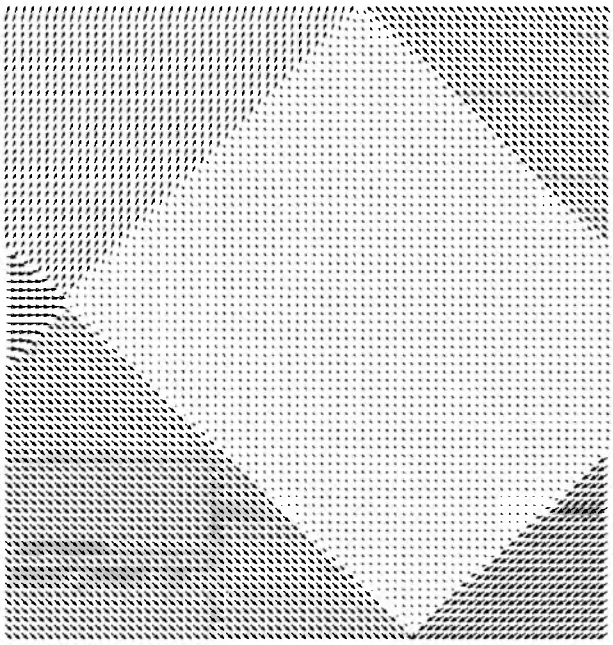

*Figure 5.* Velocity field in representative mesovolume at fragmentation.

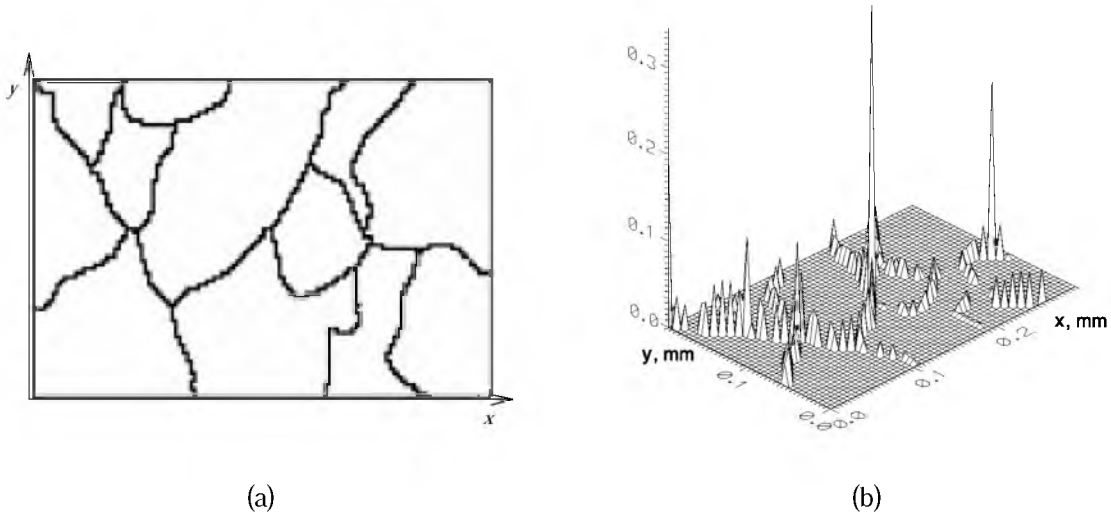


*Figure 6.* Reference structure of a mesovolume of Al–Li alloy (a) and space distribution of plastic energy when integral strain of the sample is 0.25 percent (b).

The following series of results is devoted to the calculations of composite materials. In this case not only strength but also elastic characteristics differ for different fragments of material's structure. In Figure 6(a) a map of mesovolume of Al–Li alloy is submitted. In its internal structure it is possible to recognize interlayers of oxides which are marked as black in Figure 6(a) and have the following parameters $\mu = 10\,\text{GPa}$, $K = 300\,\text{GPa}$, $\rho = 1\,\text{g/cm}^3$, $Y_0 = 22\,\text{MPa}$, and zones (or grains) of pure alloy which are white in Figure 6(a) and have the following parameters $\mu = 33\,\text{GPa}$, $K = 61.6\,\text{GPa}$, $\rho = 2.5\,\text{g/cm}^3$, $Y_0 = 250\,\text{MPa}$.

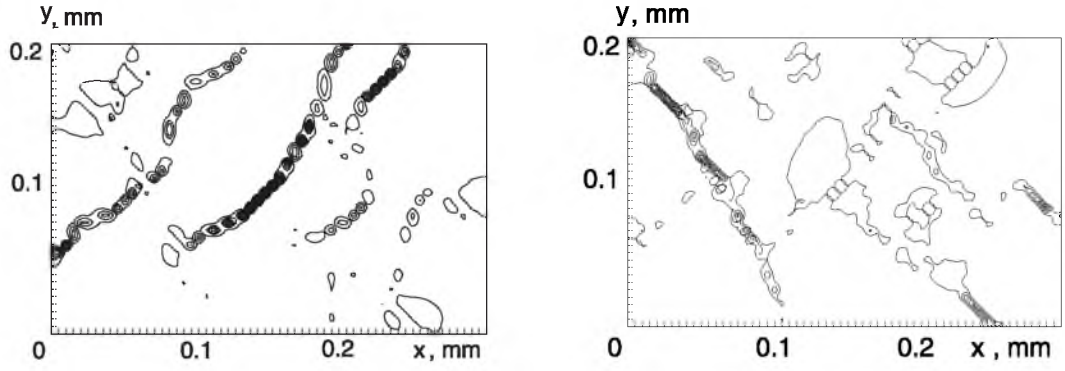


(a) (b)

*Figure 7.* Contour maps for positive (a) and negative (b) values of rotations in deformed mesovolume of Al–Li alloy.

The computation grid contains 121 × 81 nodes with initial space step 2.5 $\mu$m. The oxides have low strength characteristics and plastic deformations start to develop in them earlier. The deformation appears localized in the zones of layers. Thus, when integral strain of the sample is equal to 0.1 percent the local strain can reach 10 percent. Heterogeneous fields of stress and strain in the regions close to the interfaces cause large local rotations in the joints of fragments, which cover material of interlayers and grains partially. In Figure 7 one can see that these rotations of local areas are disposed along the interfaces with different orientation. Positive rotations are located along the interlayers with left-hand inclination whereas the negative ones are located along the interlayers with right-hand inclination in relation to the deformation axis. Though crack generation was not allowed here this calculation shows that such an internal structure with continuous oxide layers don't realize sufficient plasticity of the material and leads to it's brittle behavior.

The last example of calculations shows deformation behavior of a ceramic composite with TiC inclusions and TiNi matrix up to it's failure. Here we consider fracture with taking into account the appearance of material discontinuities. Cracks are simulated in an explicit form by splitting the computational grid nodes, so use was made of an algorithm of Lagrange grid nodes splitting (Gridneva and Nemirovich-Danchenko, 1983). An integral fracture criterion based on the damage accumulation principle was adopted for generation and growth of cracks. It has the form

$$\alpha = \int_{t_0}^{t_f} \frac{(\sigma^* - \sigma_0)^\lambda}{R}\,\mathrm{d}t, \quad \text{if } \sigma^* > \sigma_0, \tag{15}$$

where $\sigma_0$, $\lambda$, $R$ are the material constants, $\sigma^*$ is the effective stress and $0 \leqslant \alpha \leqslant 1$ is a damage parameter. The materials parameters used in the computation are presented in Table 1. The continuous contact conditions were set at the interfaces 'matrix-inclusion'. The computation grid contains 40 × 60 nodes with initial space step 1 $\mu$m.

Figure 8 shows the result of calculation for the case of the boundary conditions which are schematically presented as velocities applied on the boundary of the mesovolume. In the mesovolume of the composite under complex loading (shear + tension) a system of micro-

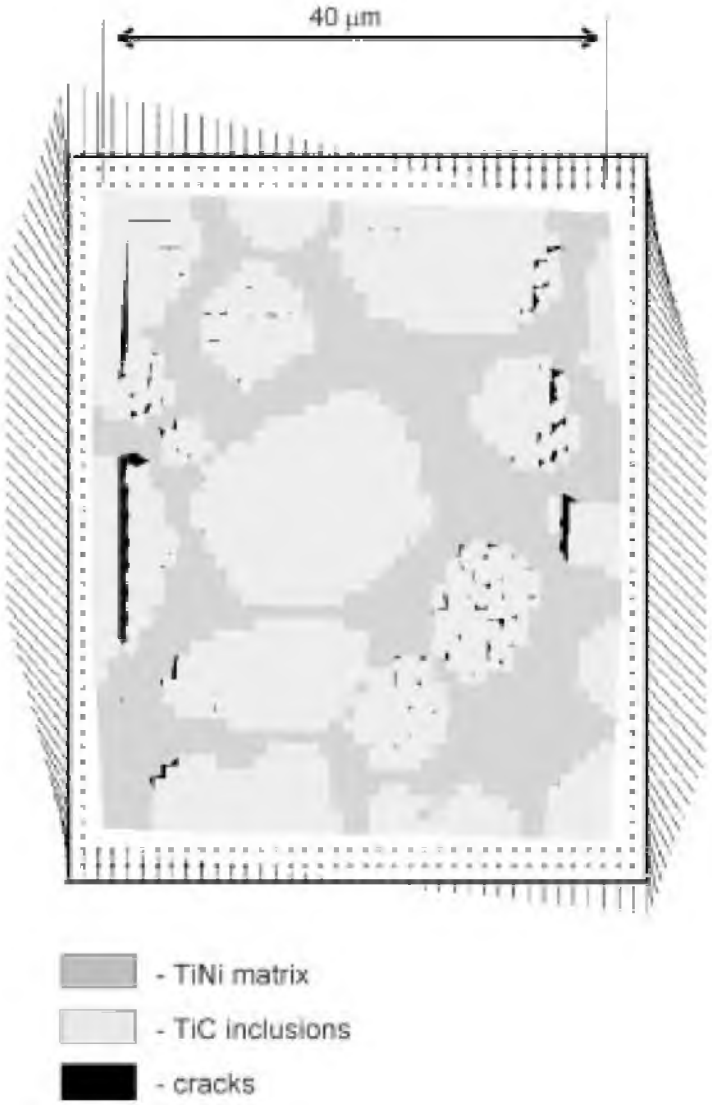


*Figure 8.* An example of simulation of mesocracks formation at the stage of large plastic deformation in the composite material with plastic matrix and brittle inclusions.

cracks appears. Here, the plastic matrix transmits loading to the brittle inclusions that crack while shear bands is forming in the matrix.

*Table 1.* Materials properties for TiNi–TiC composite.

| Material | $\rho$, g/cm$^3$ | $K$, GPa | $\mu$, GPa | $Y_0$, GPa | $\sigma_0$, GPa | $\lambda$ | $R$ |
|---|---|---|---|---|---|---|---|
| Inclusion | 4.91 | 122.0 | 188.5 | 3.0 | 0.15 | 0.82 | 1.11 |
| Matrix | 6.45 | 39.3 | 28.46 | 0.15 | 0.15 | 0.82 | 0.777 |
| Interface | | | | | 0.1 | 0.82 | 1.11 |

## 4. Conclusion

Thus, heterogeneous stressed state is typical for deformation of mesovolumes of a structurally inhomogeneous material. This is due to the stress concentrators of various nature and scale (interfaces between fragments of internal structure, feature of the shape, and etc.). In these conditions the plastic deformations proceed heterogeneously as well. They arise in the region of stress concentration and in the elements of structure with the least strength. Then, the bands of localized shear are formed where plastic strain much exceed average strain. Significant change in values of shears and rotations making the tensor of plastic distortion is marked in these bands, rotations being more sensitive to the localization of deformation. The sign of rotations depends on the orientation of the band concerning the axis of deformation. With localization of plastic deformations the material fragmentation occurs accompanied by the formation of bulk structural elements which move as a whole.

Note that the material properties at micro and mesolevels differ from the ones at the macroscale. But, unfortunately, they are not known from experiments now. Nevertheless, another values of these constants will give another quantitative, but not qualitative results in calculation. So, as we studied model samples, it did not matter quantitative values but qualitative effects did.

So, it is possible to simulate numerically localized plastic strain of meso scale in the frameworks of classic elastic-plastic model by taking into account the heterogeneous inner structure of a material in explicit form and stress concentrators of various nature.

## Acknowledgements

Support from the Russian Foundation for Basic Research through the project number 96-01-00902 is gratefully acknowledged.

## References

Dève, H., Harren, S., McCullough, C. and Asaro, R.J., (1988). Micro and macroscopic aspects of shear band formation in internally nitrided single crystals of Fe–Ti–Mn alloys. *Acta Metallurgica* **36**(2), 341–365.

Dong, M. and Schmauder, S. (1996). Transverse mechanical behaviour of fiber reinforced composites – FE modelling with embedded cell models. *Computational Materials Science* **5**, 53–66.

Gridneva, V.A. and Nemirovich-Danchenko, M.M. (1983). Method of grid nodes splitting for calculations of solids fracture, Dep. in VINITI, Tomsk, No. 3258, (in Russian).

Harren, S.V., Dève, H.E. and Asaro, R.J. (1988). Shear band formation in plane strain compression. *Acta Metallurgica* **36**(9), 2435–2480.

Nadai, A. (1950). Theory of flow and fracture of solids, Vol. 1, 2nd ed., McGraw-Hill, New York.

Panin, V.E. (ed.), (1990). Structural levels of plastic deformation and fracture, Nauka Publishing, Novosibirsk, (in Russian).

Panin, V.E. (ed.), (1998). Physical mesomechanics of heterogeneous media and computer-aided design of materials, Cambridge International Science Publishing, Cambridge.

Panin, V.E., Makarov, P.V., Nemirovich-Danchenko, M.M., Demidov, V.N., Smolin, I.Y. and Cherepanov, O.I. (1995). Methodology of computer-aided design of materials with specified strength characteristics. (Edited by V.E. Panin). *Physical Mesomechanics and Computer-Aided Design of Materials*, Vol. 2, Nauka Publishing, Novosibirsk. 3–76 (in Russian).

Panin, V.E. (1995). Physical Mesomechanics of plastic deformation and experimental results obtained by optical methods, *Journal of the Japan Society of Applied Physics* **9**, 888–894.

Panin, V.E., Zuev, L.B., Danilov, V.I., Makarov, P.V., Egorushkin, V.E., Gorbatenko, V.V., Hida, Y. and Yoshida, S. (1993). Method and apparatus for nondestructive testing of the mechanical behaviour of solid state objects under loading, Patent No. 93002731, Ruspatent, Moscow.

Soppa, E., Amos, D., Schmauder, S. and Bischoff, E. (1998). The influence of second phase and/or grain orientations on deformation patterns in a Ag polycrystal and in Ag/Ni composites. *Computational Materials Science* 13, 168–176.

Wilkins, M.L. (1964). Calculations of elastic-plastic flow. (Edited by B. Alder, S. Fernbach and M. Rotenberg), *Methods in Computational Physics*, Vol. 3, Academic Press, New York, 211–263.

Wilkins, M.L. and Guinan, M.W. (1976). Plane stress calculations with a two dimensional elastic-plastic computer program, UCRL-77251.